Effect of carbon content on the mechanical properties of ternary boron-nitrogen-carbon compound

M Pal Chowdhury, S Dalui, B R Chakraborty[a], A Mukherjee[b] & A K Pal[*]

Department of Instrumentation Science, USIC Building, Jadavpur University, Calcuttta 700 032

[a]National Physical Laboratory, New Delhi

[b]Central Glass & Ceramic Research Institute, Calcutta 700 032

*E-mail: msakp2002@yahoo.co.in

BNC films have been deposited on Si (100) and fused silica substrates by inductively coupled plasma chemical vapour deposition (ICP-CVD) technique using a mixture of borane-ammonia, nitrogen and methane as precursor gases. Carbon content in the films is varied by changing the concentration of methane in the precursor gases. The films are amorphous in nature. The films, thus, deposited have been characterized by using Fourier Transform Infrared Spectroscopy (FTIR), X-ray diffraction and Secondary Ion Mass Spectroscopy (SIMS). Microstructural information has been obtained from SEM studies. Microhardness has been seen to decrease with the increase in carbon content and the highest microhardness observed in these films has been found to be~5.3 GPa.

Keywords: BNC films, Hard coatings, Chemical vapour deposition

1 Introduction

Boron-nitrogen-carbon (BNC) compounds are emerging as promising materials of technological interest due to their favourable properties for various device applications[1-5]. Ternary phases $B_xC_yN_z$ have been intensively studied in recent years for superior mechanical (superhardness), chemical (oxidation protection), electrical and optical properties. Boron nitride and carbon being isostructural and isoelectronic, possibility of depositing a stable ternary compound like BC_xN having equal number of boron and nitrogen atoms conforming charge neutrality was studied intensively. In contrast, the synthesis of BCN films generally yielded BCN with compositions far away from BC_xN. Unlike the crystalline β-C_3N_4 and c-BN, this material is known to have the potential of retaining the superior properties of crystalline phase even when prepared in amorphous phase. Thus, ternary $B_xC_yN_z$ compounds prepared by various deposition techniques yielded BCN compounds in a wide composition range to obtain tailored material for specific applications[6,7].

In pursuit of depositing boron-carbon-nitrogen compounds, a number of methods were adopted by different workers[8-13] for synthesis of the material. Among them, reactive sputtering[8,9], laser ablation[10], plasma enhanced chemical vapour deposition[6,11], ion beam deposition[1,13] and solvothermal synthesis[12] techniques are worth mentioning. It is to be noted here that most of the techniques yielded films with soft phases and hexagonal structure, while techniques using high temperature and high-pressure (HPHT) yielded predominant cubic phase[13] material. Plasma assisted CVD (PACVD) technique has also proved to be useful for obtaining BCN coatings with superior mechanical and tribological properties when deposited at lower deposition temperatures. But there are not many studies dealing with the modulation of mechanical properties with the introduction of carbon in c-BN lattice.

In the present study, BCN films have been synthesized by inductively coupled plasma chemical vapor deposition (ICP-CVD) at 623 K by using borane-ammonia, nitrogen and methane as precursor gases. The variation of mechanical properties with the introduction of carbon in c-BN lattice has been studied critically. Ion species present at the plasma/substrate interface are recorded by optical emission spectroscopy (OES) measurements.

2 Experimental Details

B-C-N films were deposited onto Si (100) and fused silica substrates at 623 K by using an inductively coupled plasma CVD system. The

experimental jig consisted of a stainless steel base-chamber (6 inch diam, 8 inch high) to which a quartz reaction chamber (3 inch diam,10 inch long) could be fitted vertically. The base-chamber had appropriate connectors for vacuum system, vacuum gauges, hot emissive probe and window for optical emission spectrometer (OES). The OES comprised of an optical fiber to collect the optical signals from the source (here plasma) to be analyzed by using a spectrometer (UV–VIS–NIR) and a charge-coupled device (CCD) array detector. The substrate holder along with heating elements and thermocouple were introduced from the bottom of the base chamber. Borane-ammonia vapour, methane, argon and nitrogen gases were introduced in the plasma chamber by using appropriate mass flow meters. The system could be evacuated to a pressure of 10^{-6} torr. The Si and fused silica substrates were clamped to a stainless steel support plate which contained a complete heating assembly consisting of a tungsten zig-zag filament. The temperature of the substrate was controlled and monitored by an electronic on/off temperature controller with a thermocouple acting as the sensing element.

A mixture of methane and argon was used as carbon containing precursor while borane-ammonia vapour and nitrogen were utilized as the source for boron and nitrogen respectively. The above mixture was cracked by utilizing a r.f. generator (13.56 MHz; 1 kW) with matching network. The films were deposited at a chamber pressure ~ 0.4 mbar without applying any intentional substrate bias but a self-bias of 15 V was found to be generated during deposition. The deposition time was ~3 h and the resultant film thickness was ~0.5 μm. FTIR studies were carried out in the range 400-4000 cm^{-1} by using an IR spectrometer (Nicolet, Magna-IR). The film texture was recorded by Scanning Electron Microscope (SEM) (Hitachi S-2300) while the structure of the films was analyzed by XRD (Seifert 3000P). Secondary Ion Mass Spectrometry (SIMS, MIQ 256, CAMECA-RIBER) was used for tracing the impurities in these films. The primary ion source used here was Ga^+ at 4 nA current with 25 keV primary energy.

The hardness measurements were carried out by using a depth sensing indentometer FISCHERSCOPE H100CXY$_p$ with a XY programmable stage utilizing low load range between 1 and 30 mN so as to ensure that the maximum depth of penetration of the indenter does not exceed 10% of the film thickness.

3 Results and Discussion

BCN films were grown on Si (100) and fused silica substrates kept at ~623 K by ICP-CVD technique using borane-ammonia, nitrogen, argon and methane in appropriate proportions as precursor material. Relative amounts of borane-ammonia, argon and nitrogen were kept constant at the critical values required for the deposition of BN films with assured c-BN content >98%[14]. It was observed that c-BN content reached its maximum (>98%) when the ratio of $(BH_3\text{-}NH_3)$: (N_2+Ar) was 1:6. The N_2:Ar ratio utilized here was 1.2:1.

Constant flow rates for borane-ammonia and nitrogen were maintained in this study for the deposition of B-C-N films. Amount of carbon incorporated in the c-BN lattice was controlled by the amount of methane introduced in the chamber for which a mixture of methane and argon was introduced at different flow rates varying from 12 to 82 sccm in the system. No visible colour change was observed for films deposited on Si substrate while the fused silica substrate became light yellow after the deposition of the BCN film. The BCN films deposited as above were amorphous in nature as determined by X-ray diffraction (XRD) analysis (not shown here) and the SEM micrograph (Fig. 1) indicated a smooth surface resembling for amorphous materials.

3.1 FTIR studies

FTIR is generally considered to be an effective tool to get a qualitative insight about the possibility of formation of ternary phases. Here, the peak position is determined by the bond strength and the mass of the bonded atoms. Shifts due to chemical environment of the atoms generally result in the shift of peak position.
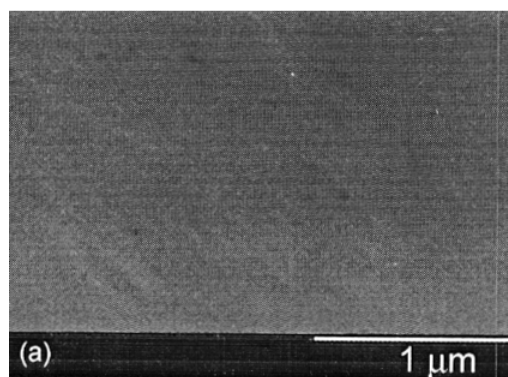

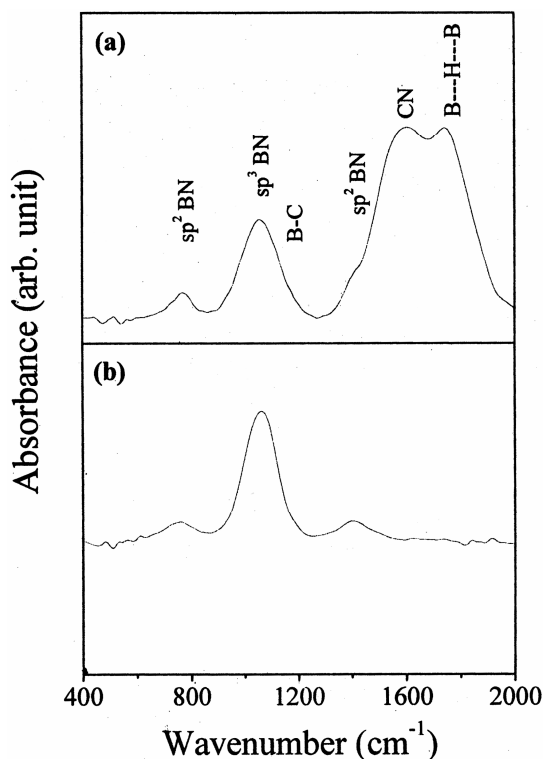Fig. 1 — SEM micrograph of a 12% carbon content BCN sample

Fig. 2 — FTIR spectra of: (a) a representative BCN film
(BCN-54), (b) BN films

The phase separation of carbon and BN would modulate the hybridization[15] in the BCN compound and the possibility of phase separation is generally enhanced at higher deposition temperature. Thus, in most deposition techniques utilized so far, the films are generally carbon doped BN (BN:C). It is now well accepted that for realization of a properly hybridized BCN compound, simultaneous formation of CN and BC during the synthesis is a prerequisite[16].

FTIR spectra for a representative BCN film (~12% carbon content) are shown in Fig. 2a. FTIR spectrum for c-BN film (>90% c-BN content) is also shown in Fig. 2b for the sake of comparison. The spectrum for c-BN is dominated (Fig. 2b) by a very strong peak at ~1060 cm^{-1} related to B-N stretching for c-BN followed by two very weak peaks at ~1370 and 780 cm^{-1} for B-N stretching and B-N-B bending modes respectively for h-BN. No significant peaks were observed in the higher wave number. As carbon was introduced in the c-BN lattice, additional characteristic peaks related to BCN compound appeared. The intensity of the absorption band around 1060 cm^{-1} for the B-N stretching mode of sp^3 bonded B-N decreased. Presence of B-C bond could be overlapped with sp^3 bonded BN absorption peak. The

broad features appearing in the FTIR absorption spectra between 1300 and 1700 cm^{-1} may arise due to stretching modes for the CN double and single bonds. The vibrational modes for CH$_2$ and CH$_3$ may[7-19] also appear in the same range of energy and would overlap with the stretching modes for CN. It may also be noted that a distinct signature of B–H–B bridge bonds[19] appeared in the region 1600–2000 cm^{-1} for all the films deposited here. It was observed that with the increase in methane flow rate the intensity of the peak for sp^3 bonded BN decreased and the broad feature for CN stretching modes became prominent.

3.2 SIMS studies

SIMS combines excellent sensitivity with the capability of analyzing all elements including hydrogen. A typical mass spectrum of the secondary ions emerging from a BCN film is shown in Fig. 3. SIMS profile clearly shows the presence of carbon while the presence of nitrogen is overlapped with the possible presence of CH$_2$. The lines for the B isotopes (^{10}B, ^{11}B) are clearly seen in this figure. One may observe the presence of oxygen in the films. This may arise due to the presence of physisorbed oxygen incorporated during the transport of the films for SIMS study when the films were exposed to atmospheric oxygen for considerable time. The other mass peaks may be related to the substrate (Si) and other contaminants from the deposition chamber. It may be noted here that the relative sensitivity factors (RSFs) of Na, K, and Ca are very high compared to those for constituents like B, C and N. Thus, the actual amount of these alkali metal impurities will be very small and expected to be approximately at parts per million level. Relative amount of boron, nitrogen
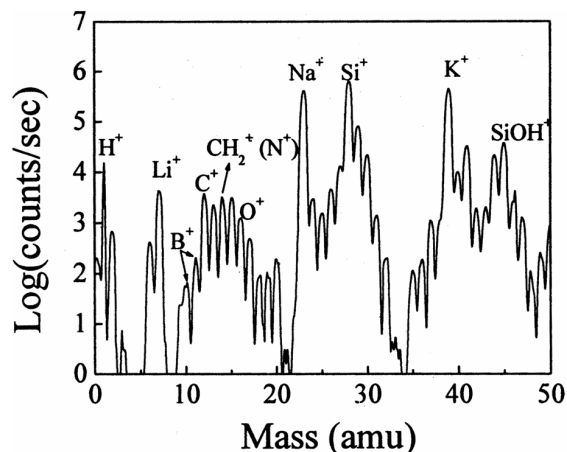

Fig. 3 — General SIMS profile of a BCN film with
lower carbon content

and carbon was ascertained from the SIMS study by using the sensitivity factors of individual elements and counts for pure B, N and C determined simultaneously during SIMS analysis.

3.3 Plasma diagnostics by OES

It would be interesting to study the relative intensities of the plasma species present at the plasma/substrate interface when methane was introduced to incorporate carbon in the BN lattice as nature, amount and energies of different plasma species present at the plasma/substrate interface are known to modulate the synthesis in CVD techniques.

In the synthesis of boron nitride and boron carbonitride by CVD technique, hydrogen plays an important role[20]. It is known that when the plasma contains excess hydrogen, substrate bias may not be required for obtaining sp^3 bonded BN as predominant phase. Direct dissociation of borane-ammonia resulted in the presence of hydrogen plasma species (Fig. 4a) like H_α and H_β at 656 and 486 nm respectively[21,22]. Presence of second positive system (SPS) of N_2 was also observed in the above plasma. It may be noted here that the presence of BH as well as B lines were not observed in the plasma since the intensity of these lines were quite small compared to that of SPS of N_2 lines[22]. Besides direct dissociation of borane ammonia, the borane ammonia transformation due to hydrogen abstraction in the plasma may occur according to the following chemical reaction[20]:

$$BH_3NH_3 + 2H^\cdot = BH_2NH_2 + 2H_2$$

$$BH_3NH_3 + 4H^\cdot = BHNH + 4H_2$$
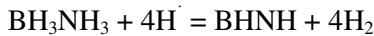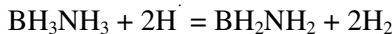
The CH_4 plasma has been examined by OES in a separate experiment. It was found that in addition to CH lines at 387 nm[22] and 431 nm, spectral lines for H_α, H_β were also observed in the plasma obtained by cracking CH_4 alone. A strong line for H_2 at 613.5 nm[22] was also found to dominate the above spectra.

The molar ratio of CH_4/Ar was also varied from 1/40 to 1/5 in the chamber during the deposition of BCN. It would be interesting to note that no hydrogen lines were detected by OES and strong lines for nitrogen species and CH and CN bands[21] at ~390 and ~ 416.7 nm, respectively, were found to dominate the OES spectra (Fig. 4b). The relative intensity of the lines for CH and CN was seen to be dependent on the molar ratio of CH_4/Ar. The above variation is shown in Fig. 5 which indicated that the intensity of CH band
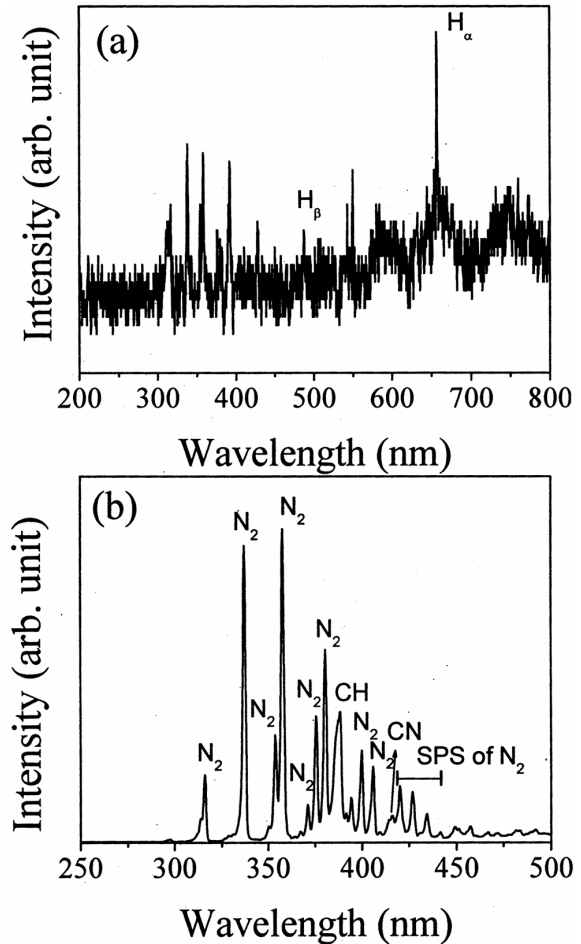

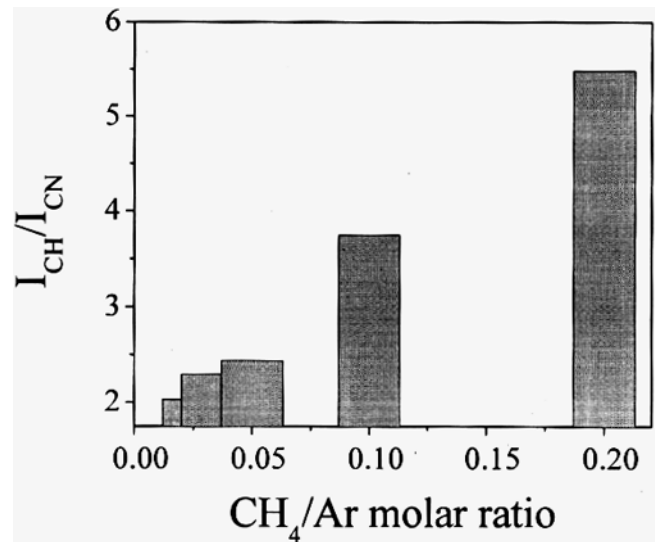Fig. 4 — Representative OES spectra for: (a) Borane-ammonia only, (b) plasma during the growth of BCN film

Fig. 5 — Variation of CH/CN OES intensity ratio I_{CH}/I_{CN} with CH_4/Ar molar ratio
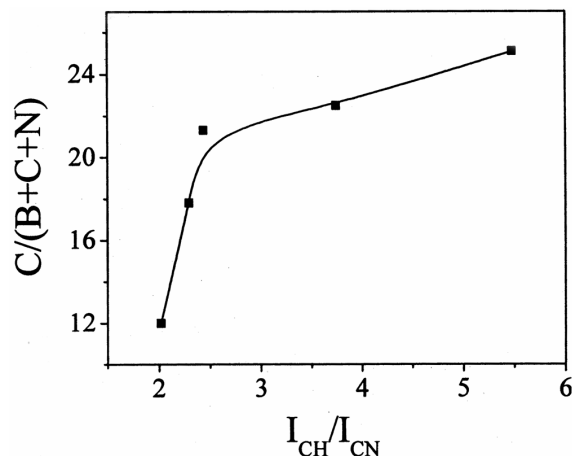
Fig. 6 — Variation of carbon content with CH/CN OES intensity ratio I_{CH}/I_{CN} for BCN films

increased much faster than that of CN band. The carbon content in the films tended to saturate beyond a critical molar ratio of CH₄/Ar as indicated from the dependence of carbon content with the relative intensity of the lines for CH and CN as shown in Fig. 6.

In addition to the direct electronic dissociation of hydrogen ($H_2 + e^- \rightarrow 2H + e^-$), the Ar emission line at 420 nm may reveal the active roles played by argon in the dissociation process of hydrogen[23-26]:

$$Ar^+ + H_2 \rightarrow ArH^+ + H$$

$$Ar\,(^3p_2) + H_2 \rightarrow Ar\,(^1s_0) + 2H$$
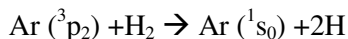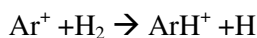
This would culminate in an increase in atomic hydrogen in the plasma due to the presence of Ar. The relative deposition rate of sp^3 bonded BN can be enhanced owing to selective etching of sp^2 bonded BN from the surface of the growing film by excited hydrogen species in the plasma. Further, atomic hydrogen would also facilitate the removal of graphitic or amorphous carbon from the surface of the deposited films. Thus, the interaction between BH₂NH or BNH radicals, nitrogen species along with CN and CH radicals would lead to the formation of the ternary compound of B-C-N on the substrate surface.

3.4 Hardness measurements

The hardness of the B-C-N films was determined from the indentation curve (Fig. 7) by extrapolating the unloading curve from the maximum applied load P_{max} to zero. A linear extrapolation of the unloading curve between 70 and 100% of P_{max}, utilized by

Doerner and Nix[27], was used here while the corrected indentation depth, h_{cor} was ascertained from the power-law fitting of the unloading curve[28,29].

Variations of hardness and Young's modulus of the B-C-N films as a function of carbon content are presented in Fig. 8. It could be seen that both the hardness and the Young's modulus decreased as the carbon content in the films was increased form 12 to 25%. This may be ascribed due to the presence of more covalent B-C bonds compared to the B-N bonds at lower carbon content in the films. Incorporation of carbon in sp^3-bonded BN led to amorphous character of the B-C-N films. This was also reflected in the relative increase in B-C bonds and different carbon-nitrogen bonds which were also apparent in the FTIR spectra. In other words, the films with higher percentage of carbon would exhibit lesser rigidity. It may further be noted that the B-C-N film with carbon content ~12% showed a hardness of 4.12 GPa. As the carbon content in the films increased to 25%, the
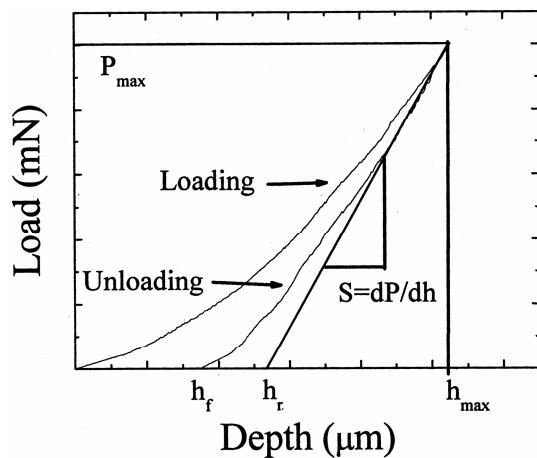

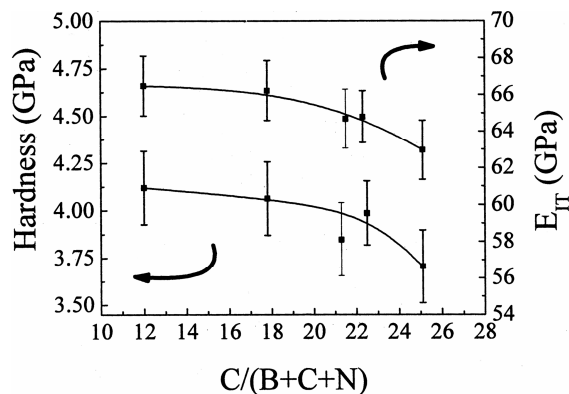Fig. 7 — Schematic diagram of the load-depth pattern in a DSI experiment

Fig. 8 — Variation of Hardness and Young's modulud (E_{IT}) with carbon content for BCN films

hardness value declined by about 10% to 3.71 GPa. Similarly, the Young's modulus also decreased from a value of about 67 GPa for films with 12% carbon content by about 5.3% to ~ 63 GPa for films containing 25% carbon. The films were comparatively soft compared to the hardness value obtained by Linss *et al.*[30] which could be ascribed due to large hydrogen content in the films as indicated by FTIR and SIMS studies.

The load dependence of the hardness was also studied here and a representative plot for a B-C-N film (BCN-54) with the lowest carbon content of 12% and highest hardness of 4.12 GPa is shown in (Fig. 9). It may be observed that the hardness decreased exponentially as the load was increased and then tended to saturate with the increase in the load. At an applied low load of ~1 mN, the hardness as recorded by the DSI technique was as high as about 5.3 GPa. However, as the indentation load was increased, the hardness decreased till ~7.5 mN beyond which it tended to saturate ~4 GPa. This variation indicates that there could be an indentation size effect (ISE) modulating the experimentally observed hardness.

Variation of elastic deformation energy (W_e) and energy absorbed in permanent plastic deformation process (W_p) with carbon content in the B-C-N films studied here are shown in Fig. 10. The observed variation could qualitatively be understood in terms of a simplistic energy based principle which assumed that there was no significant influence on the deformation processes arising out of the substrate and the film/substrate interface during the DSI experiments. If the total work (energy) of indentation (W_t) of the thin film is assumed to be a sum total of elastic deformation energy requirement (W_e) and energy absorbed in permanent plastic deformation process (W_p) only, then accepting a simplified view that there is no significant loss of energy in this whole process, one can assume $W_t = W_e + W_p$. This would mean that the films with larger carbon content would indicate greater W_p component while the elastic deformation energy (W_e) would be less and vice versa. Indeed, the experimentally observed variation of the elastic deformation energy (W_e) and the energy absorbed in permanent plastic deformation processes (W_p) with carbon content in the B-C-N films seem to support the above description (Fig. 9).

The static indentation plastic hardness is the pressure that would cause permanent plastic deformation[28,31,32]:
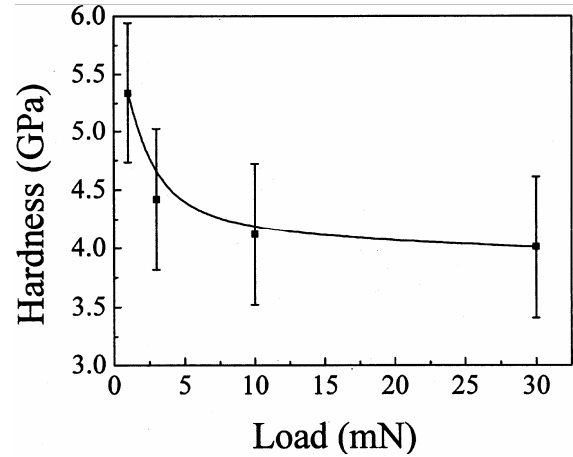

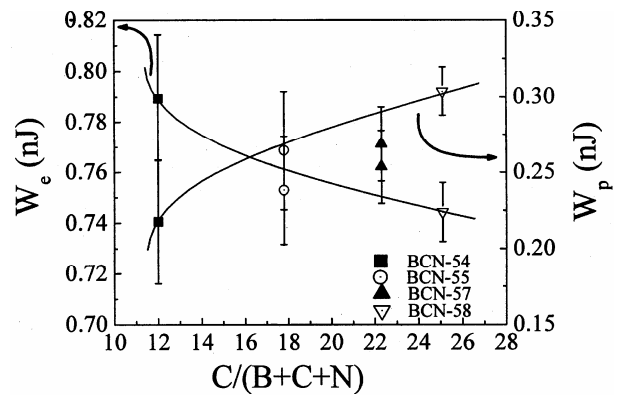Fig. 9 — Variation of hardness with load for BCN film (e.g. BCN-54) with 12% carbon content in the film

Fig.10 — Variation of deformation energy (W_e) and energy absorbed in permanent plastic deformation process (W_p) with carbon content for BCN films

$$H = L/A_C \qquad \ldots(1)$$

Here, A_C is the contact area (in m^2) between the indenter and the material under the applied load L (in Newton) giving the hardness in Pascal. For an ideal conical indenter, such as a Vicker's pyramid, hardness is independent of applied force[28,31,32] and is calculated from Eq. (1). In practice, the conical indenter has finite tip radius and the L/A_C value increases as the applied force decreases. The two possibilities that may arise are: (a) the nominal contact area underestimates the real one and/or (b) the pressure under indentation does not reach the flow stress. Small volume under test for thin film specimens is another possible reason of ISE. At low load, the possibility of finding a critical flaw would decrease and this might limit the strength of the material significantly.

4 Conclusions

The BCN films were synthesized by inductively coupled plasma CVD using borane-ammonia, N_2 and CH_4 as precursors. All the films were amorphous in nature as determined by XRD analysis. The films were characterized by SEM, SIMS and FTIR studies. The FTIR spectra of BCN films show the presence of sp^3 bonded BN, sp^2 bonded BN, CN single and double bonds in the films. Both the hardness and the Young's modulus were found to decrease with increased carbon content in the films. This may be due to the presence of more covalent B-C bonding compared to the B-N bonding at lower carbon content in the films. Incorporation of carbon in sp^3-bonded BN led to amorphous character of the B-C-N films. The relative increase in B-C and different carbon-nitrogen bonding has also been reflected in the FTIR spectra. Load dependence of the hardness indicated that there could be an indentation size effect (ISE) modulating the experimentally observed hardness.

Acknowledgement

References

1   Ying Z F, Yu D, Ling H, Xu N, Lu Y F, Sun J & Wu J D, *Diam Relat Mater*, 16 (2007) 1579.

2   Morant C, Prieto P, Bareno J, Sanz J M & Elizalde E, *Thin Solid Films*, 515 (2006) 207.

3   Okada K, Kimura C & Sugino T, *Diam Relat Mater*, 15 (2006) 1000.

4   Miyake S, Wang M & Kim J, *Nanotechnology*, 17 (2006) 1607.

5   Oates T W H, Ryves L, Burgmann F A, Abendroth B, Bilek M M M, McKenzie D R & McCulloch D G, *Diam Relat Mater*, 14 (2005) 1395.

6   Dekempeneer E H A, Meneve J, Kuypers S & Smeets J, *Thin Solid Films*, 281-282 (1996) 331.

7   Liu L, Zhao Y, Tao Y, Yang D, Ma H & Li Y, *Appl Surf Sc*, 253 (2006) 439.

8   Liu L, Wang Y, Feng K, Li Y, Li W, Zhao C & Zhao Y, *Appl Surf Sc*, 252 (2006) 4185.

9   Byon E, Son M, Lee K H, Nam K S, Hara N & Sugimoto K, *Electrochim Acta*, 51 (2006) 2662.

10   Kaeaguchi M & Kawashima T, *J Chem Soc, Chem Commun,* 14 (1993) 1133.

11   Perrone P, Carricato A, Luches A, Dinescu M, Ghica C, Sandu V & Andrei A, *Appl Surf Sc*, 133 (1998) 239.

12   Sun G, Liu Z Y, Zhou Z, He J, Yu D & Tian Y, *Diam Relat Mater*, 15 (2006) 1659.

13   Sasaki T, Akaishi M, Yamaoka S, Fujiki Y & Oikawa T, *Chem Mater*, 5 (1993) 695.

14   Chowdhury M P & Pal A K, *J Phys D: Appl Phys*, 37 (2004) 261.

15   Moore A W, Strong S L, Doll G L, Dresselhaus M S, Spain I L, Bowers C W & Piraux L, *J Appl Phys*, 65 (1989) 5109.

16   Liu A Y, Wentzcovitch R M & Cohen M L, *Phys Rev B*, 39 (1989) 1760.

17   Setsuhara Y, Sakawa Y, Shoji T, Kumagai M & Mikaye S, *Surf Coat Technol*, 142 (2001) 874.

18   Onate J I, Garcia A, Bellido V & Viviente J L, *Surf Coat Technol*, 49 (1991) 548.

19   Lehmann W J & Shapiro I, *Spectrochim Acta*, 17 (1961) 396.

20   Konyashin I, Loeffler J, Bill J & Aldinger F, *Thin Solid Films*, 308-309 (1997) 101.

21   Rudolph R N & Moore J H, *Plasma Chem Plasma Process*, 10 (1990) 451.

22   Pearse R W B & Gaydon A G, *The Identification of Molecular Spectra*, (Chapman and Hall, London) 1976, pp 217.

23   Capitelli M, Dilonardo M & Molinari E, *Chem Phys*, 20 (1977) 417.

24   Dotan J & Lindinger W, *J Chem Phys*, 76 (1982) 4972.

25   Schaffnit C, Thomas L, Rossi F, Hugon R & Pauleeau Y, *Surf Coat Technol*, 98 (1998) 1262.

26   Setsuhara Y, Sakawa Y, Shoji T, Kumagai M & Mikaye S, *Surf Coat Technol*,   142-144 (2001) 874.

27   Doerner M F & Nix W D, *J Mater Res*, 1 (1986) 601.

28   Veprek S, Mukherjee S, Karvankova P, Männling H D, He J L, Moto K, Prochazka J & Argon A S, *Thin Solid Films*, 436 (2003) 220.

29   Oliver W C & Pharr G M, *J Mater Res*, 7 (1992) 1564.

30   Linss V, Barzola-Quiquia J, Ha¨ussler P & Richter F, *Thin Solid Films*, 467 (2004) 66.

31   Tabor D, *The hardness of metals*, (Clarendon Press, Oxford) 1951, pp 115-119.

32   Meyer E, Zeitschrift des Vereines Deutscher Ingenieure, 52 (1908) 645.